Comparison of Recorded and Computed Earthquake Response of Arch Dams

Anil K. Chopra
University of California, Berkeley

Jinting Wang
Tsinghua University, Beijing, China

15 WCEE
LISBOA 2012

SUMMARY:
Utilizing a recently developed linear analysis procedure and computer software, which includes dam-water-foundation interaction effects and recognizes the semi-unbounded extent of rock and impounded water domains, the response of two arch dams to spatially-varying ground motion recorded during past earthquake is investigated. Computed responses are compared with recorded motions.

Keywords: Arch Dams, Earthquake Response, Ground Motions

1. INTRODUCTION

The response of two arch dams to spatially-varying ground motions recorded during earthquakes is computed by a recently developed linear analysis procedure that includes dam-water-foundation rock interaction effects and recognizes the semi-unbounded extent of the rock and impounded water domains [Wang and Chopra, 2008]. The computed responses are compared with recorded responses to demonstrate the effectiveness of the analysis procedure.

2. EARTHQUAKE RESPONSE OF MAUVOISIN DAM

2.1 Mauvoisin Dam and Earthquake Records

Located in the Swiss Alps, Mauvoisin Dam is a 250-m-high double curvature arch dam [Fig. 1(a)]. The dam was built to a height of 237 m during 1951-1957, and raised to its present height during 1989-1991. The base of the dam is at El. 1726 m above sea level and its crest at El. 1976 m. It is composed of 28 blocks for a total crest length of 520 m. The thickness of the crown cantilever decreases from 53.5 m at the base to 12 m at the crest [Fig. 1(b)].

Figure 2 shows an array of 12 three-component strong-motion (SM) accelerographs operating at the dam since 1993. Accelerographs SM01-SM05 are located inside the upper gallery, 14 m below the crest; accelerographs SM06-SM08 are located at mid-height, and accelerographs SM09-SM11 are located at the base elevation. Installed in tunnels, accelerographs SM09 and SM11 are located essentially vertically below SM01 and SM05, respectively; SM10 is located at the base of the dam. Accelerographs SM01, SM06, SM08, and SM05 are located at the dam-foundation rock interface; SM01 and SM06 are located on the left side of the canyon (viewed from upstream), and SM05 and SM08 on the right side of the canyon. Accelerograph SM0F is located in the free field 600 m downstream of the dam at El. 1840, i.e., 114 m above the dam base on the left side of the canyon.

Figure 1. Mauvoisin Dam, Switzerland: (a) view from the downstream; and (b) cross-section of crown cantilever

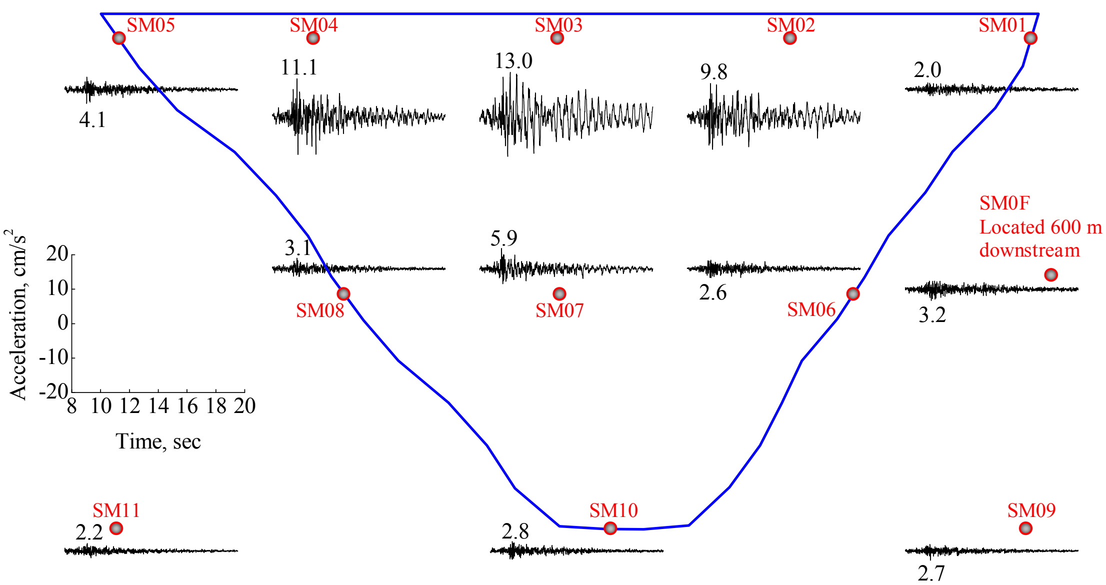

Figure 2. Recorded motions in stream direction; accelerations are in cm/sec^2; peak values are noted

Motions of Mauvoisin Dam during the magnitude 4.6 Valpelline earthquake of 31 March 1996 centered 13 km away from the dam, were recorded by the accelerograph array. At the time of the earthquake, the water level was at El.1864, i.e., 112 m below the crest of the dam. The stream components of motions recorded at the accelerograph locations are shown in Fig. 2; for brevity, similar figures for the cross-stream and vertical components are not included, but are available in Chopra and Wang [2008]. Although the motions are very weak, these records provide a useful set of data about the spatial variations of ground motions around the canyon along the dam-foundation rock interface, thus providing an opportunity to investigate the influence of spatial variations in ground motion on response of the dam.

2.2 System Analyzed

Figure 3 presents a finite element model of the dam that includes one hundred forty-five 8-node thick shell elements and a total of 468 nodes, the finite element mesh for the irregular region of the fluid domain and the boundary element mesh at the dam-rock interface. The foundation rock domain is treated as semi-unbounded and the fluid domain as unbounded in the upstream direction. The water in the model is now at El. 1870 m (compared to the actual El. 1863 m). Based on correlation of computed response with ambient vibration data and known concrete and rock properties, Proulx et al. [2001] selected parameter values for the dam-water-foundation rock system as follows: Concrete: elastic modulus = 36 GPa, Poisson's ratio = 0.2, and unit mass = 2400 kg/m^3; foundation rock: elastic modulus = 72 GPa, Poisson's ratio = 0.25, and unit mass = 2500 kg/m^3; water: unit mass = 1000 kg/ m^3 and wave velocity = 1438 m/s; and wave reflection coefficient at the reservoir boundary = 0.9. These material properties (elastic properties and unit weight) of the dam concrete and rock were maintained here with one minor exception: a lower elastic modulus of 25 GPa was assigned to the uppermost 12.5 m of the dam, the part raised in 1991; this value comes from test data for the new concrete [Proulx et al., 2004].

Data obtained from three concrete arch dams in the Swiss Alps provides a basis to choose damping values for earthquake analysis of these dams. Ambient vibration tests led to a viscous damping ratio of approximately 2–3% in the lower vibration modes of Mauvoisin Dam [9], and similar values were obtained for the 130-m-high Punt-del-Gall Dam [3]. Forced vibration tests of Emosson Dam also resulted in approximately 2–3% damping [10], which is the same as for Mauvoisin Dam. Although ambient vibration data for damping are usually considered less precise than forced vibration data, the damping value for Mauvoisin Dam seems reliable, as the concrete and rock properties at the site are similar to those found at Emosson Dam.

Damping values for the dam alone and foundation rock separately were selected to achieve a viscous damping ratio of about 2% for the overall dam-water-foundation rock system. For this purpose, frequency response functions for the response at the crest center due to spatially-uniform excitation at the interface in the stream and cross-stream directions were determined for several combinations of damping in the dam and in foundation rock. In one such combination, we assumed a viscous damping ratio of 1% (in all vibration modes) of the dam alone and 3% for the foundation rock, and determined from the resonance curve—by the half-power bandwidth method—the viscous damping ratio to be 2.2% in the first symmetric mode and 1.5% in the first-anti-symmetric mode, indicating that the chosen damping values for concrete and rock provide an overall damping of about 2% for the dam-water-foundation rock system, which is consistent with experimental data.

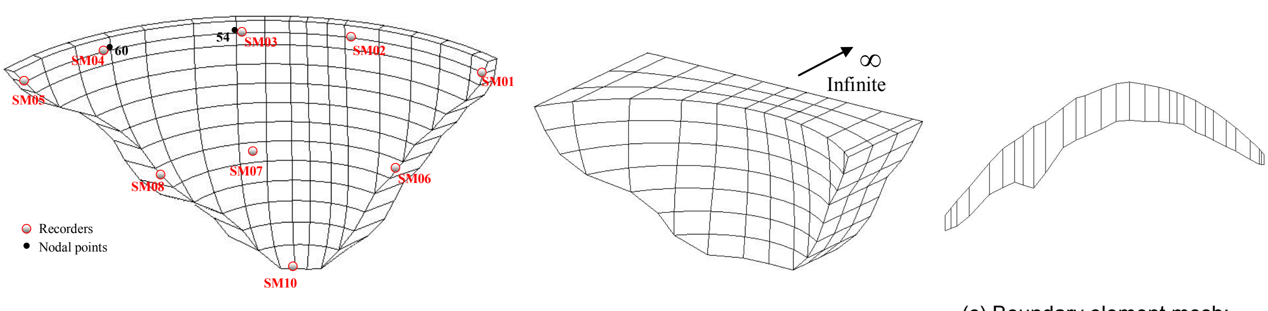

(a) Finite element model: dam

(b) Finite element model: reservoir

(c) Boundary element mesh: dam-foundation rock interface

Figure 3. EACD-3D-2008 model for Mauvoisin Dam

2.3 Comparison of Computed and Recorded Responses

The response of the dam to the recorded spatially-varying excitation is determined by the analysis procedure presented in Chopra and Wang [2008]. The computed displacement responses of the dam are reasonably similar to the recorded displacements, but the agreement is far from perfect. The peak values of the computed displacements in the stream direction—the direction of the largest response—are very close to the recorded value (Fig. 4). While the computed value at node 54 is 92% of the value recorded at SM03 (i.e., they differ by 8%), and the computed value at node 60 is 101% of the value recorded at SM04 (i.e., the two differ by 1%), the computed displacement histories do not agree as well. Although the computed displacement history is very close to that recorded over some time segments, the two differ significantly during other time segments (Fig. 4), e.g., the computed displacement at node 54 in the stream direction is very close to that recorded at SM03 during 14-18 sec, but the two differ significantly over other time segments.

Recognizing that the recorded ground motions provide an incomplete description of the earthquake excitation [Chopra and Wang, 2010], and that no attempts were made to adjust the published data for parameter values for the mass and stiffness properties of the concrete and rock [Proulx et al., 2004], the agreement between computed and recorded motions is modestly good.

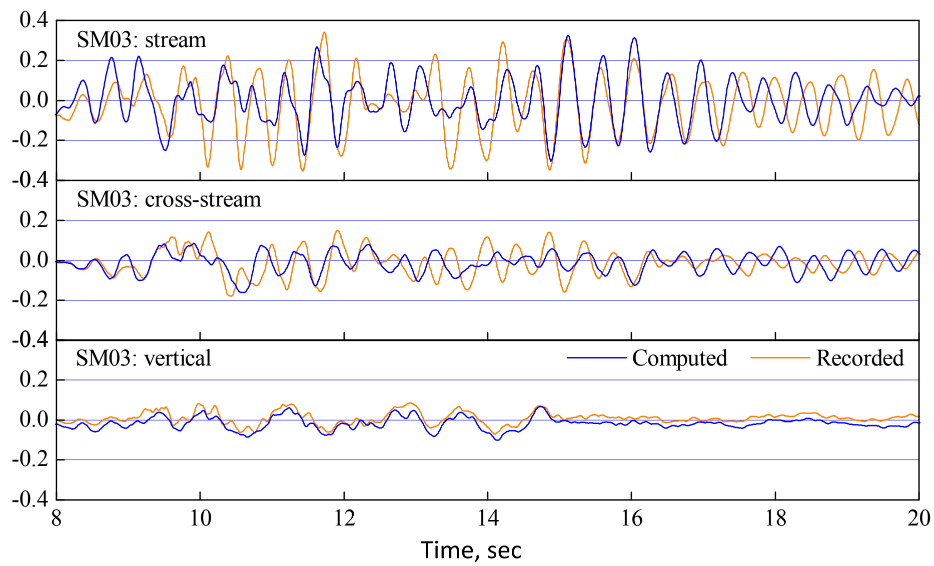

Figure 4. Comparison of recorded and computed displacements—stream, cross-stream and vertical components—at crest center (SM03); computed responses are for node 54 (near SM03)

3. RESPONSE OF PACOIMA DAM TO TWO EARTHQUAKES

3.1 Pacoima Dam and Earthquake Records

Located in the San Gabriel Mountains near Los Angeles, Pacoima Dam is a 113-m-high concrete arch dam, with a crest length of 180 m [Fig. 5(a)]. Completed in 1928, the dam varies in the thickness from about 3 m at the crest to 30 m at the base. A concrete thrust block supports the dam at the left abutment [Fig. 5(b)]. The eleven contraction joints in the dam body have beveled keys that are 30 cm deep.

(a)

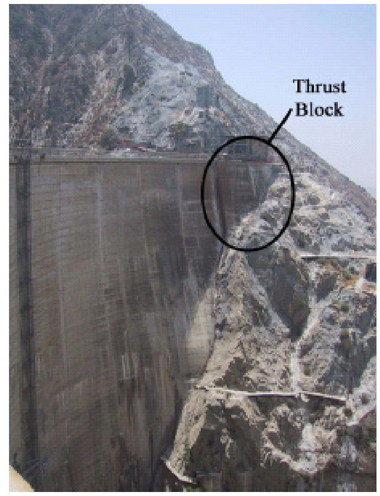

(b)

Figure 5. Pacoima Arch Dam: (a) Dam; (b) Left abutment

The array of accelerographs shown in Fig. 6 is designed to record 17 channels of motions. Three-component accelerographs are located at the base, left abutment, right abutment, and center of the crest, and one-component accelerographs are located at five locations on the dam body.

This instrument array recorded the motions during the magnitude 6.7 Northridge earthquake of 17 January 1994, with its epicenter about 18 km southwest of the dam and a focal depth of 19 km. The water surface was 40 m below the crest during the earthquake. Peak horizontal accelerations ranged from 0.5*g* at the base of the dam to about 2.0*g* on the canyon sidewalls near the crest. Spatial variations in the ground motions in both amplitude and phase from the bottom of the canyon to the top and from one side of the canyon to the other were striking. Because of the intense ground shaking, the dam sustained significant damage that was repaired. The accelerometer array was also repaired and upgraded.

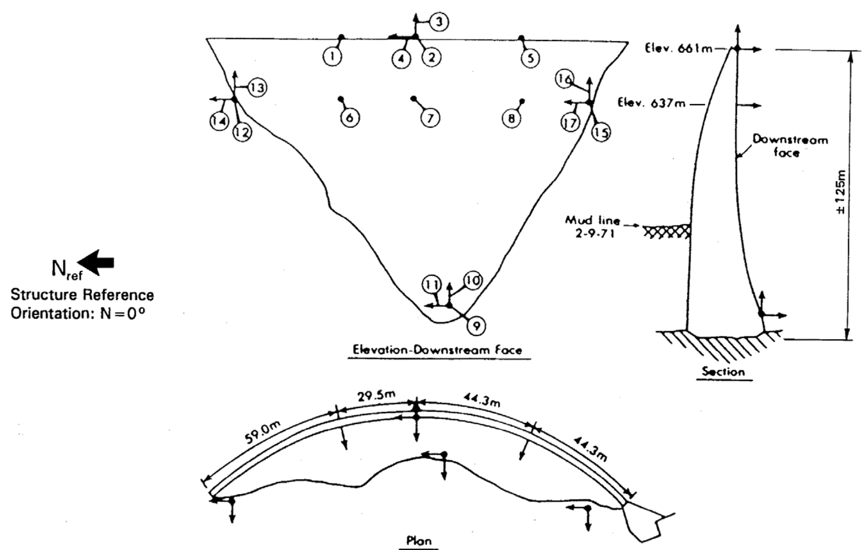

Figure 6. Accelerograph locations at Pacoima Dam (CSMIP *Report OSMS 01-02*)

On 13 January 2001 a magnitude 4.3 earthquake occurred, with its epicenter about 6 km south of Pacoima Dam and focal depth of about 9 km. The water level was 41 m below the crest at the time of this earthquake. The stream (or radial) component of the recorded motions is presented in Fig. 7; the cross-stream (or tangential) and vertical components are available in Chopra and Wang [2008]. Spatial variation in ground motions along the dam-foundation rock interface is evident. In the stream direction, the peak acceleration of 13 cm/sec^2 at the base is amplified to 43 and 34 cm/sec^2 at the left and right abutments, respectively (Fig. 7). In the cross-stream direction, the peak acceleration of 20 cm/sec^2 at the base is amplified to 95 cm/sec^2 at the left abutment and to 50 cm/sec^2 at the right abutment; the large difference between the amplitudes of the motions at the two abutments is striking.

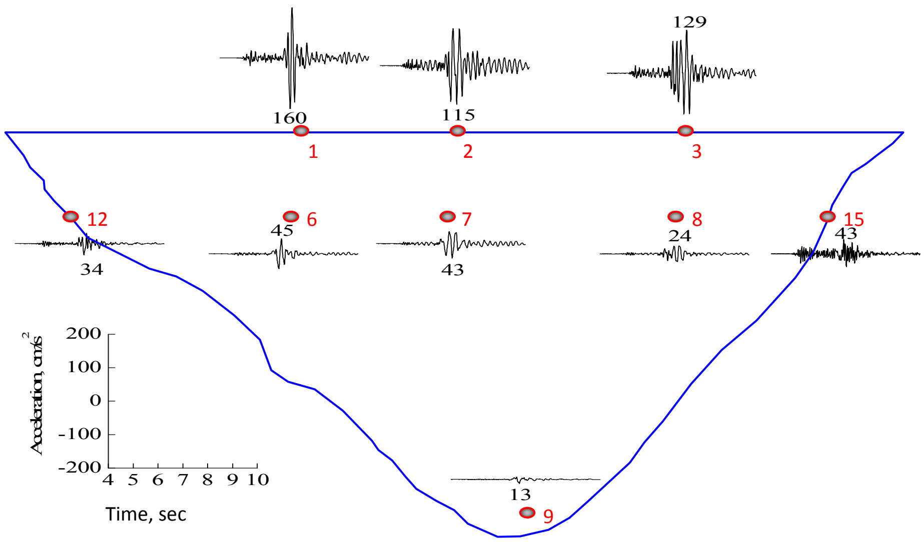

Figure 7. Recorded accelerations (cm/sec^2) in stream or radial direction at Channels 1-3, 6-8, 9, 12, and 15 during the January 13, 2001, earthquake

The cross-stream (or tangential) component of the motions "recorded" during the 1994 earthquake are presented in Fig. 8; the stream (or radial) and vertical components are available in Chopra and Wang [2008]. Spatial variation in ground motions along the dam-foundation rock interface is evident. In the stream direction, the peak acceleration of 429 cm/sec^2 at the base is amplified by a factor of approximately two at the abutments. In the cross-stream direction, the peak acceleration of 518 cm/sec^2 at the base is amplified to 1317 and 744 cm/sec^2 at the left and right abutments. The time variation of motions at the two abutments are similar, but the difference in amplitude is striking; in contrast, the stream motions at the two abutments are similar.

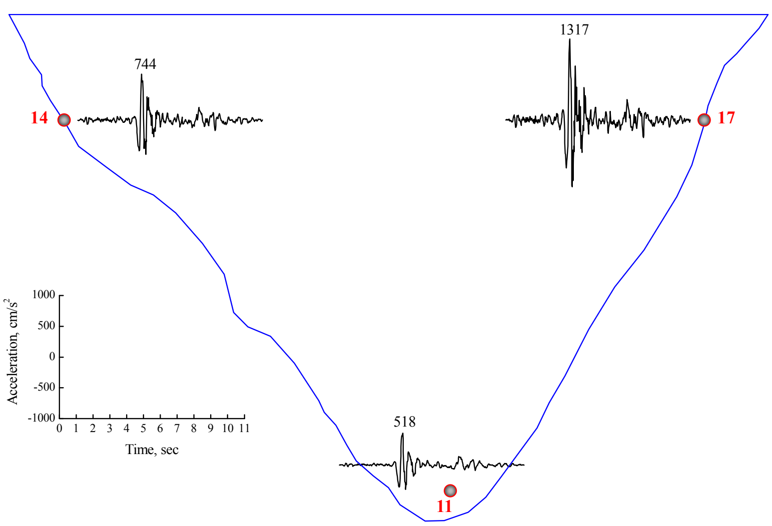

Figure 8. Accelerations (cm/sec^2) generated by Alves [2004] in cross-stream direction at Channels 11, 14, and 17 to represent motions during Northridge earthquake

3.2 System Analyzed

Figure 9 shows the finite element model for Pacoima Dam, the finite element mesh for the irregular region of the fluid domain, and the boundary element mesh at the dam-rock interface; the foundation rock domain is treated as semi-unbounded, and the fluid domain as unbounded in the upstream direction; see Chopra and Wang [2008] for a detailed description.

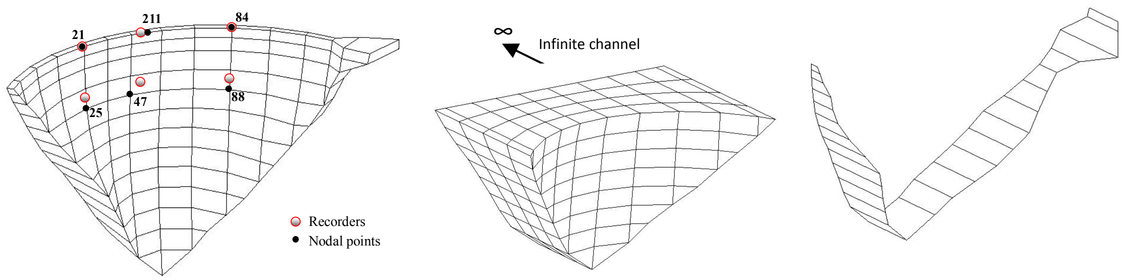

(a) Finite element model: dam (b) Finite element model: reservoir (c) Boundary element mesh: dam-foundation rock interface

Figure 9. EACD-3D-2008 model for Pacoima Dam

The elastic moduli used for the dam and foundation rock are 21.9 GPa (3180 ksi) and 10.9 GPa (1575 ksi), respectively. These properties were established by calibration of a finite element model to approximate the modal properties determined by system identification using the earthquake records of January 13, 2001 [Alves, 2004]. The other properties were based in part on material tests: unit weight of concrete equal to 22.3 kN/m^3 (142 lb/ft^3) of rock equal to 25.9 kN/m^3 (165 lb/ft^3), and of water equal to 9.8 kN/m^3 (62.4 lb/ft^3); shear wave velocity in water = 1438 m/sec (4720 ft/sec). Although Alves' model neglected the mass of foundation rock and compressibility of water, no attempt was made to refine his values for concrete and rock moduli for use in the EACD-3D-2008 model, which included foundation rock mass and water compressibility.

Damping values for the dam alone and foundation rock were selected for the EACD-3D-2008 model to achieve damping in the overall dam-water-foundation-rock system consistent with the aforementioned system identification studies that had led to viscous damping ratios of 6.2% in the first symmetric vibration mode and 6.6% in the first anti-symmetric vibration mode [Alves, 2004]. For this purpose, the frequency response functions due to spatially-uniform excitation were computed for several combinations of damping in the dam and foundation rock. In one such combination, a viscous damping ratio of 2% (in all vibration modes) of the dam alone and 4% for the foundation rock was assumed. Determined from the resonance-curve—by the half-power bandwidth method—the viscous damping ratio was 7.0% in the first mode and 6.7% in the first anti-symmetric mode (second mode of the dam) [Chopra and Wang, 2008], values that are close to the identified values.

3.3 13 January 2001 Earthquake

The response of the dam to the spatially-varying ground motion recorded during the 2001 earthquake was determined by the analysis procedure presented in Chopra and Wang [2008]. The computed displacements compare well the recorded displacements (Fig. 10). The time-variation of the computed displacements is close to the recorded response over its entire duration; however, the peak displacement at Channels 1 and 2 is over-estimated by 22% and 40%, respectively. Recognizing that the recorded ground motions provide only an incomplete description of the earthquake excitation, and that no attempts were made to adjust the published data [Alves, 2004] for the mass and stiffness parameters of concrete and rock, the agreement between computed and recorded displacements is satisfactory.

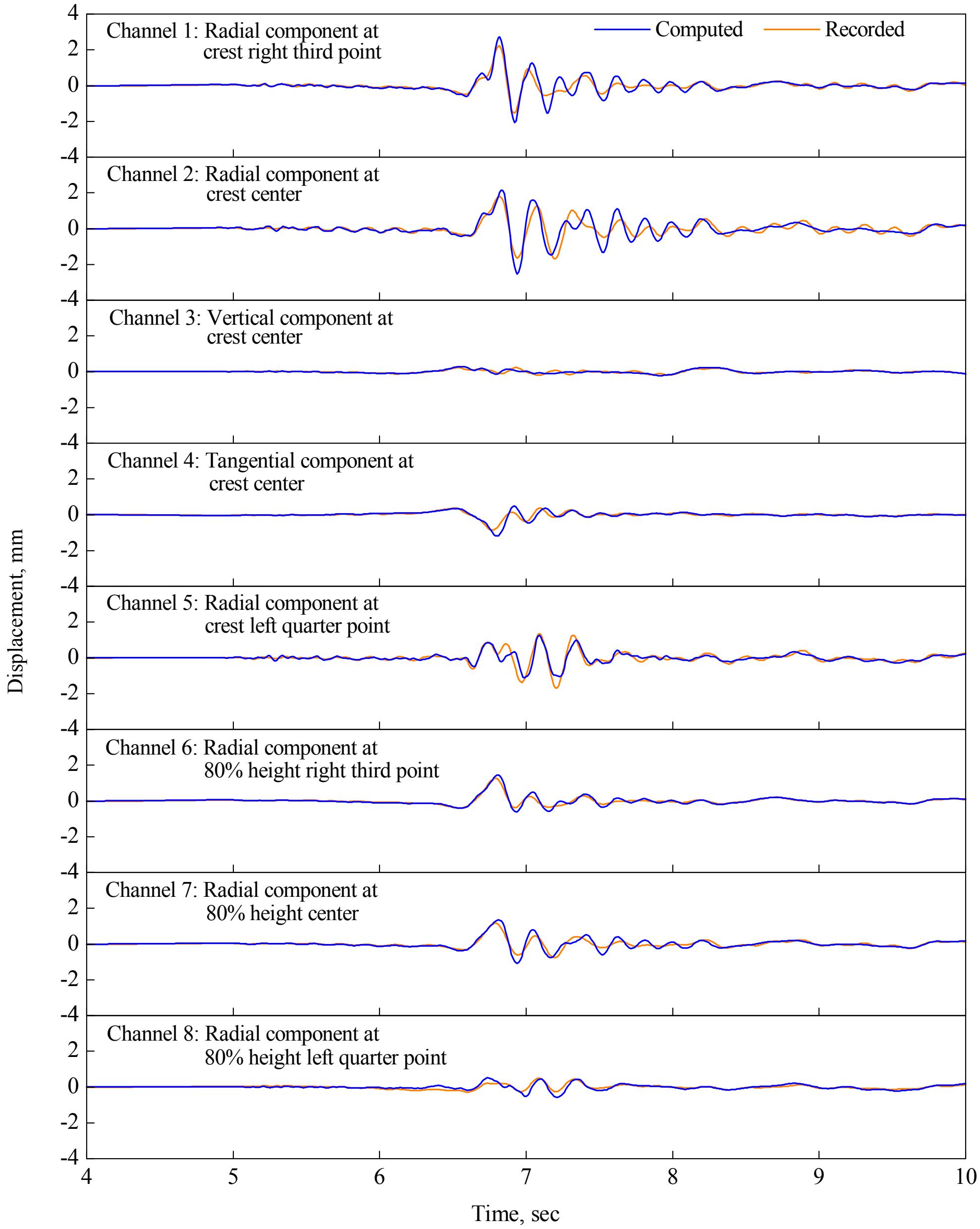

Figure 10. Comparisons of recorded and computed displacements at Channels 1-8 due to the January 13, 2001, earthquake. Computed responses is at the following nodal points: 21 (near Channel 1), 211 (near Channels 2-4), 84 (near Channel 5), 25 (near Channel 6), 47 (near Channel 7), and 88 (near Channel 8)

3.4 17 January 1994 Northridge Earthquake

A direct comparison of the motions of Pacoima Dam computed by linear analysis against the motions recorded during its nonlinear response to the damaging 1994 earthquake is not meaningful. Instead, the stresses computed by linear analysis are presented to investigate if they correctly identify the zones where the dam was damaged.

Figure 11 presents the peak value of the tensile stresses in the arch direction on the downstream face; similar figures for arch and cantilever stresses on both faces of the dam are available in Chopra and Wang [2008]. Presented are the stresses due to four different excitations. The first three are spatially-uniform excitations defined by ground motion at the base of the dam (Channels 9–11), the right abutment (Channels 12–14), and the left abutment (Channels 15–17). The fourth excitation is defined as the "recorded" (and interpolated or extrapolated) spatially-varying ground motion. The distribution pattern of stresses due to the three spatially-uniform excitations is similar, although the magnitude of stresses due to ground motions recorded at the base of the dam is much smaller than those due to motions at the left or right abutment; the stresses due to the two abutment excitations are similar in magnitude. By comparing the stresses due to spatially-varying and spatially-uniform excitations, clearly the spatial variations in ground motion had profound influence on the magnitude and the distribution of arch stresses (Fig. 11).

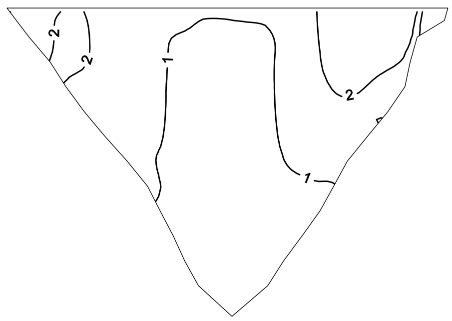

(a) Spatially-uniform excitation: Channels 09-11

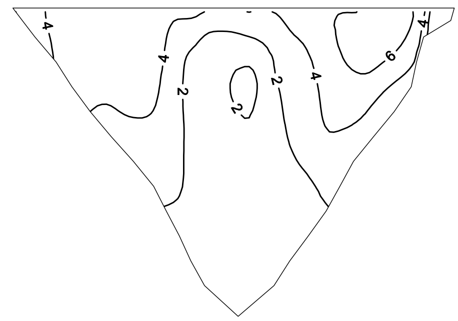

(b) Spatially-uniform excitation: Channels 12-14

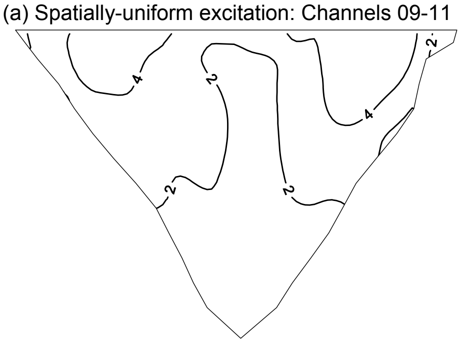

(c) Spatially-uniform excitation: Channels 15-17

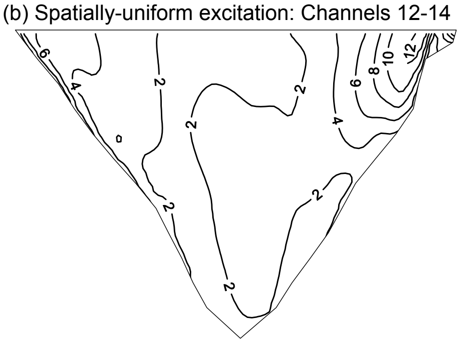

(d) Spatially-varying excitation

Figure 11. Peak values of tensile arch stress (MPa) on the downstream face due to the Northridge earthquake: (a) spatially-uniform excitation defined by Channels 09-11; (b) spatially-uniform excitation defined by Channels 12-14; (c) spatially-uniform excitation defined by Channels 15-17; and (d) spatially-varying excitation

Figure 12. Joint opened and cracks occurred in the thrust block of Pacoima Dam during the Northridge earthquake

Because these stresses were computed by linear analysis, they are not indicative of actual stresses that developed in the dam because vertical contraction joints opened and cracking occurred during the earthquake. The large arch stresses computed in the thrust block between the dam and the left abutment and the portion of the dam adjacent to the thrust block (see Fig. 11 and additional figures in Chopra and Wang [2008]) suggests that cracking would occur in these areas, which is what actually happened during the earthquake; cracking is visible in Fig. 12. Clearly, the three analyses that ignored spatial variations in ground motion are unable to identify the damaged regions.

4. CONCLUSIONS

The earthquake responses of two dams computed by a linear analysis procedure—which included dam-water-foundation rock interaction effects, recognized the semi-bounded extent of the rock and impounded water domains—and considered the spatial variations are in good agreement with the recorded motions and observed damage recorded during the two earthquakes.

REFERENCES

Alves, S.W. (2004). Nonlinear analysis of Pacoima dam with spatially non-uniform ground motion. *Report No. EERL 2004-11*, California Institute of Technology, Pasadena, California.

Chopra, A.K., and Wang, J. (2008). Analysis and response of concrete arch dams including dam-water-foundation rock interaction to spatially-varying ground motions, *Report No. UCB/EERC*-2008/03, Earthquake Engineering Research Center, University of California, Berkeley, California, 124 pgs.

Chopra, A.K., and Wang, J. (2010). Earthquake response of arch dams to spatially varying ground motions, *Earthquake Engineering and Structural Dynamics*, **39:3**,887–906.

Proulx, J., Paultre, P., Rheault, J., and Robert, Y. (2001). An experimental investigation of water level effects on the dynamic properties of a large arch dam, *Earthquake Engineering and Structural Dynamics*, **30**,1147–1166.

Proulx, J., Darbre, G.R., and Kamileris, N. (2004). Analytical and experimental investigation of damping in arch dams based on recorded earthquake. *Proceedings*, *13th World Conference on Earthquake Engineering*, Paper No. 68, Vancouver, Canada.

Wang, J., and Chopra, A. K. (2008). A computer program for three-dimensional analysis of concrete dams subjected to spatially-varying ground motion, *Report No. UCB/EERC-2008/04*, Earthquake Engineering Research Center, University of California, Berkeley, California.